

# Synthesis of $\text{Li}_3\text{Cu}_2\text{SbO}_6$ , a New Partially Ordered Rock Salt Structure

J. M. S. Skakle,\* M. A. Castellanos R.,† S. Trujillo Tovar,† and A. R. West\*

\*Department of Chemistry, University of Aberdeen, Meston Walk, Aberdeen AB24 3UE, United Kingdom; and

†Universidad Nacional Autonoma de Mexico, Facultad de Quimica, Mexico DF04510, Mexico

Received August 22, 1996; in revised form February 12, 1997; accepted February 18, 1997

The new phase  $\text{Li}_3\text{Cu}_2\text{SbO}_6$ , synthesised by solid state reaction at  $1000^\circ\text{C}$ , is monoclinic,  $a=5.4659(1)$ ,  $b=8.7272(2)$ ,  $c=9.7807(3)$  Å,  $\beta=95.080(2)^\circ$ , space group  $C2/c$ , and has a partially ordered rock salt structure related to the ordered structure of  $\text{Li}_2\text{TiO}_3$  by additional cation order: Ti sites are occupied by Cu and Sb in ordered fashion; Li sites contain Li/Cu in two sets, but with nonstatistical occupancy, and Li. Bond lengths show a Jahn–Teller elongation of  $\text{CuO}_6$  octahedra consistent with magnetic susceptibility data that indicate paramagnetic  $\text{Cu}^{2+}$  ions.  $\text{Li}_3\text{Cu}_2\text{SbO}_6$  shows a low level of electronic conductivity.

© 1997 Academic Press

## INTRODUCTION

The rock salt structure is exhibited by a number of simple oxides and also by a variety of oxides containing more than one cation. In the latter case the cations can be disordered to give the simple face centred cubic structure or can exhibit a range of cation ordering arrangements. Recently, a family of structures,  $\text{Li}_3\text{M}_2\text{XO}_6$ :  $M = \text{Mg, Co, Ni}$ ;  $X = \text{Nb, Ta, Sb}$ , has been shown to exhibit partial cation order but with an unusual nonstatistical occupancy of the Li/M sites [1, 2]: there are three sets of sites for the Li/M cations and the distribution over these sites is nonrandom and varies with the nature of  $M$  (and  $X$ ). The partial cation order appears to be an equilibrium arrangement at low temperatures, although in the case of  $\text{Li}_3\text{Ni}_2\text{NbO}_6$ , the cation arrangement becomes increasingly statistical over the range  $1100$ – $1300^\circ\text{C}$ , as the structure undergoes a continuous (partial) order–disorder transition [3].

In spite of the apparent simplicity of the rock salt structure, there appears to be a rich diversity of superstructure arrangements. The present work is part of a program to synthesize new Cu-containing rock salt structures. We report a new phase with a novel, partially ordered superstructure.

## EXPERIMENTAL

The new phase,  $\text{Li}_3\text{Cu}_2\text{SbO}_6$ , was synthesized during a study of phase formation between  $\text{Li}_3\text{SbO}_4$  and  $\text{CuO}$  [4].

All compositions on this join have the requisite 1:1 stoichiometry for the rock salt structure and indeed, we have recently confirmed  $\text{Li}_3\text{SbO}_4$  to have an ordered, rock salt structure [5]. Starting materials were Analar grade  $\text{Li}_2\text{CO}_3$ ,  $\text{Sb}_2\text{O}_5$ , and  $\text{CuO}$ . These were dried, weighed out to give 5–10 g reaction mixtures, and fired in Au foil boats, initially at  $650^\circ\text{C}$  for a few hours to expel  $\text{CO}_2$ , and finally at  $1025^\circ\text{C}$  for 12 h to complete the reaction. Samples were slowly cooled ( $1^\circ\text{C}/\text{min}$ ) to room temperature. In addition, because of the order/disorder transition observed in  $\text{Li}_3\text{Ni}_2\text{NbO}_6$  [3], small portions of the sample were (a) quenched onto a brass plate from the reaction temperature or (b) annealed at  $400^\circ\text{C}$  in flowing oxygen. No differences in the structure and ordering of the quenched, annealed, and slowly cooled samples were observed. A phase diagram study of the join  $\text{Li}_3\text{SbO}_4$ – $\text{CuO}$  has shown  $\text{Li}_3\text{Cu}_2\text{SbO}_6$  to be cation stoichiometric, with no evidence of solid solution formation [6].

Initial phase analysis used a Siemens D5000 X-ray diffractometer; for accurate measurements and structure determination a Stoe Stadi/P psd-based system was used with  $\text{CuK}\alpha_1$  radiation. Data for indexing and Rietveld refinement were collected over the range  $10^\circ$ – $110^\circ 2\theta$ , step size  $0.5^\circ 2\theta$  (psd resolution  $0.02^\circ$ ), with a total counting time of 10 h. The diffraction pattern of the new phase,  $\text{Li}_3\text{Cu}_2\text{SbO}_6$ , was indexed satisfactorily using the autoindexing program INDEX, which is part of the Stoe software package.

Conductivity measurements were carried out on a sintered pellet with Au electrodes using a Hewlett–Packard 4192 impedance instrument. Magnetic measurements were performed on a Lakeshore ac5000 susceptometer,  $f = 667$  Hz and  $H = 2 \text{ Am}^{-1}$ .

## RESULTS

Automatic indexing on the first 20 lines of the powder pattern of  $\text{Li}_3\text{Cu}_2\text{SbO}_6$  gave a monoclinic unit cell of dimensions  $a = 5.463$ ,  $b = 8.727$ ,  $c = 9.789$  Å,  $\beta = 95.16^\circ$ . Lattice refinement using the Stoe program LATREF resulted in a unit cell of  $a = 5.4644(5)$ ,  $b = 8.7215(8)$ ,  $c = 9.7760(9)$  Å,  $\beta = 95.095(8)^\circ$ ; the fully indexed powder pattern is given in

**TABLE 1**  
**Fully Indexed Powder Pattern for  $\text{Li}_3\text{Cu}_2\text{SbO}_6$ :  $a=5.4644(5)\text{\AA}$ ,  $b=8.7215(8)\text{\AA}$ ,  $c=9.7760(9)\text{\AA}$ ,  $\beta=95.095(8)^\circ$**

<i>h</i>	<i>k</i>	<i>l</i>	Int.	<i>d</i> (obs)	<i>d</i> (calc)	<i>h</i>	<i>k</i>	<i>l</i>	Int.	<i>d</i> (obs)	<i>d</i> (calc)
0	0	2	100.0	4.8643	4.8687	-1	3	5	7.5	1.5835	1.5831
0	2	0	20.0	4.3589	4.3607	-3	3	1	15.2	1.5381	1.5383
-1	1	1	19.0	4.2960	4.2994	2	0	5	14.0	1.5208	1.5211
1	1	1	33.9	4.0529	4.0555	0	2	6			1.5210
0	2	2	10.4	3.2456	3.2483	1	3	5			1.5206
0	0	3			3.2458	3	3	1	7.0	1.5032	1.5029
-1	1	3	9.8	2.7542	2.7548	0	4	5	9.5	1.4526	1.4525
2	0	0	21.3	2.7200	2.7214	-3	3	3	5.3	1.4329	1.4331
-1	3	1	32.1	2.5051	2.5057	-2	4	4			1.4325
-2	0	2	12.1	2.4699	2.4708	0	6	2	3.7	1.3928	1.3928
1	3	1	25.0	2.4537	2.4546	-1	1	7	3.4	1.3602	1.3605
0	0	4	11.3	2.4342	2.4344	3	3	3	3.4	1.3518	1.3518
-1	3	2	2.5	2.3097	2.3090	2	0	6	2.4	1.3420	1.3424
2	2	0			2.3087	-4	0	2			1.3417
2	0	2	35.5	2.2896	2.2905	-4	2	2	5.0	1.2823	1.2824
0	4	0	2.3	2.1808	2.1804	2	6	0			1.2822
-2	2	2	4.0	2.1503	2.1497	-3	3	5	3.5	1.2542	1.2544
0	2	4	4.8	2.1252	2.1256	-1	3	7	2.6	1.2448	1.2448
-1	3	3	53.1	2.0551	2.0544	-3	5	2	2.4	1.2359	1.2360
2	2	2	3.7	2.0274	2.0278	2	6	2	5.0	1.2275	1.2273
0	4	2	2.1	1.9896	1.9899	0	0	8	2.3	1.2174	1.2172
1	3	3	12.8	1.9721	1.9724	1	5	6	2.2	1.1455	1.1454
-2	0	4	5.4	1.8997	1.9002	4	0	4			1.1452
3	1	0	2.3	1.7755	1.7763	-2	6	6	2.7	1.0272	1.0272
-3	1	1			1.7749	3	7	0			1.0271
2	0	4	5.2	1.7391	1.7393	3	3	7	2.3	0.9955	0.9954
3	1	1	2.3	1.7217	1.7212						
-2	4	2	2.4	1.6349	1.6348						
3	1	2	4.3	1.6232	1.6238						
0	0	6			1.6229						
2	2	4	2.1	1.6153	1.6155						

Note. Average  $\Delta(2\theta) = 0.011$ ; maximum  $\Delta(2\theta) = 0.020$ .

Table 1. Systematic absences indicated a C-centred lattice ( $hkl$ :  $h + k = 2n$ ); from a cell search on the Inorganic Crystal Structure Database (ICSD) it was found that the unit cell was similar in size to those of  $\text{Li}_2\text{TiO}_3$  and  $\text{Li}_2\text{SnO}_3$ , which are ordered rock salts crystallizing in space group  $C2/c$ . It was considered likely, therefore, that the structure of  $\text{Li}_3\text{Cu}_2\text{SbO}_6$  would be based on that of  $\text{Li}_2\text{TiO}_3$ . Atomic parameters for  $\text{Li}_2\text{TiO}_3$  were taken from Dorian and Newnham [7] and are given in Table 2a. Theoretical patterns were generated using the Stoe program THEO for  $\text{Li}_3\text{Cu}_2\text{SbO}_6$  based on possible ordered cation arrangements. None of these matched the experimental data particularly well. The most promising model was one in which Li occupied the first two positions, Li(1) and Li(2), Cu occupied the next two, Li(3) and Ti(1), and Sb the fifth, Ti(2); this refined to a final  $R$ -value ( $R_{\text{wp}}$ ) of 16.2% although the atomic parameters for the lithium atoms could not be refined. This suggested that while the basic model was correct, there was some degree of disorder in the cation sites.

The approach taken to determine the correct distribution of the cations was to use an average scattering factor for the cations based on the formula, place these average cations in each of the five crystallographic sites, and refine only the

**TABLE 2a**  
**Atomic Parameters for  $\text{Li}_2\text{TiO}_3$  Used as a Starting Model for  $\text{Li}_3\text{Cu}_2\text{SbO}_6$**

		<i>x/a</i>	<i>y/b</i>	<i>z/c</i>
Li1	8f	0.238	0.077	0.000
Li2	4d	1/4	1/4	1/2
Li3	4e	0	0.045	1/4
Ti1	4e	0	0.415	1/4
Ti2	4e	0	0.747	1/4
O1	8f	0.141	0.265	0.138
O2	8f	0.102	0.586	0.138
O3	8f	0.138	0.906	0.138

site occupancies. Calcium was taken as an approximate average of the scattering power of ( $\text{Li}_3\text{Cu}_2\text{Sb}$ ). The structure was hence treated as  $\text{Ca}_6\text{O}_6$ , with positional parameters fixed at the values for  $\text{Li}_2\text{TiO}_3$ . The refinement converged successfully to the final site occupancies shown in Table 2b; a possible interpretation of these occupancies is given in the final column, although at this stage the agreement is only approximate.

A new refinement of the structure was carried out using this deduced cation arrangement. The antimony and copper positions were refined first, followed by oxygen, lithium/copper (assuming initially a 50:50 occupancy of the Li/Cu sites), and finally, lithium sites. The thermal parameters were added one by one in the same order, and once these parameters had converged, the site occupancies for the lithium/copper sites were included. The full refinement converged to give  $R_{\text{wp}} = 4.81\%$ ; the Li occupancies of the Li/Cu sites converged to 0.595(9) for Li2 and 0.38(1) for Li3. This gives a stoichiometry of  $\text{Li}_{2.975}\text{Cu}_{2.025}\text{SbO}_6$  which is, within e.s.d.'s, equal to the nominal stoichiometry of  $\text{Li}_3\text{Cu}_2\text{SbO}_6$ . The occupancies of the Li/Cu2 and Li/Cu3 sites were then fixed at 0.6/0.4 and 0.4/0.6 respectively, and the rest of the structure refined as before. The final observed and difference profiles are shown in Fig. 1, with the crystallographic data for  $\text{Li}_3\text{Cu}_2\text{SbO}_6$  obtained by Rietveld refinement in Table 3 and a selection of bond lengths and angles in Table 4.

The cation octahedra show a range of distortions:  $\text{SbO}_6$  octahedra are largely regular with only a small variation in bond lengths and angles, as expected for a polarising species such as Sb(V). Li(1) octahedra show considerable nonsystematic distortion, with bond lengths ranging from 1.97 to 2.36 Å; similar distortions for Li environments are common in complex oxides. The Cu-containing sites are the most distorted and can be regarded as octahedra with two long apical bonds either side of a fairly regular equatorial plane. Such octahedral distortions point to a Jahn–Teller effect, characteristic of  $\text{Cu}^{2+}$  in an octahedral environment. A similar distortion is seen in mixed Li/Cu sites, consistent with

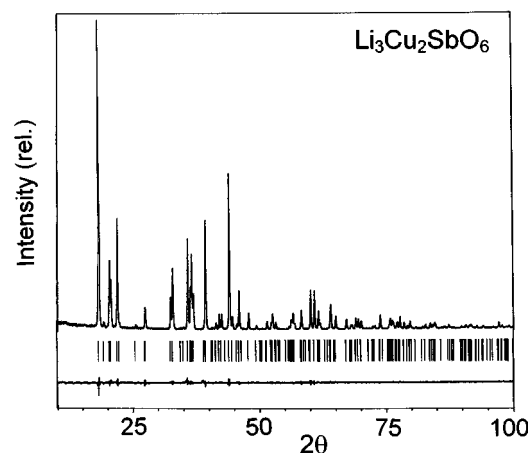


FIG. 1. Experimental X-ray powder diffraction pattern for  $\text{Li}_3\text{Cu}_2\text{SbO}_6$  with difference profile after Rietveld refinement.

the observation that Li is rather flexible in its co-ordination requirements and can adapt to the more specific requirements of Jahn–Teller active  $\text{Cu}^{2+}$ . Bond valences for the  $\text{Li}_3\text{Cu}_2\text{SbO}_6$  structure were calculated from the bond lengths using appropriate constants from Brown [8] and are given in Table 5. The values for Li and Sb are very close to the atomic valence, confirming the correctness of the structure for these ions; the rather low values for the Cu-containing sites are attributed to the Jahn–Teller distortions in the environment for these ions which lead to two anomalously long Cu–O bonds and hence a reduction in their associated bond valence.

The crystal structure of  $\text{Li}_3\text{Cu}_2\text{SbO}_6$  is a partially ordered rock salt structure derived from that of  $\text{Li}_2\text{TiO}_3$  (and  $\text{Li}_2\text{SnO}_3$ ). The cation distributions in  $\text{Li}_3\text{Cu}_2\text{SbO}_6$  and  $\text{Li}_2\text{TiO}_3$  are illustrated in Fig. 2. Within the cubic close-packed array of oxide ions, five sets of octahedral sites are occupied by the cations, two of which show partial, non-statistical occupancy of Li and Cu.

TABLE 2b  
Refined Occupancies for  $\text{Ca}_6\text{O}_6$  and Their Interpretation  
in Terms of the  $\text{Li}_3\text{Cu}_2\text{SbO}_6$  Structure

Site	No.	Occupancy	$Z^a$	
8f	Ca1	0.30	6	Li
4d	Ca2	0.69	13.8	Li/Cu
4e	Ca3	0.98	19.6	Li/Cu
4e	Ca4	1.36	27.2	Cu
4e	Ca5	2.81	56.2	Sb

<sup>a</sup> $Z$  is the effective atomic number (number of electrons), assuming that the site is fully occupied instead of being partially occupied by the average cation Ca.

TABLE 3  
Final Parameters after Rietveld Refinement for  $\text{Li}_3\text{Cu}_2\text{SbO}_6$

Site	$x/a$	$y/b$	$z/c$	$U_{\text{iso}}$ (Å <sup>2</sup> )	Occupancy	
Li1	8f	0.230(4)	0.0798(15)	−0.010(2)	0.084(3)	
Li2	4d	1/4	1/4	1/2	0.0421(10)	0.6
Cu2						0.4
Li3	4e	0	0.0785(8)	1/4	0.065(14)	0.4
Cu3						0.6
Cu4	4e	0	0.4140(4)	1/4	0.0304(6)	
Sb5	4e	0	0.7484(2)	1/4	0.0192(2)	
O1	8f	0.1785(2)	0.2378(11)	0.1434(4)	0.0444(14)	
O2	8f	0.1130(10)	0.5889(12)	0.1224(6)	0.049(2)	
O3	8f	0.0882(10)	0.9021(11)	0.1196(5)	0.031(2)	

Note.  $R_p = 2.72\%$ ;  $R_{\text{wp}} = 4.59\%$ ;  $R_{\text{Bragg}} = 1.86\%$ ;  $R_{\text{exp}} = 1.70\%$ . Spacegroup  $C2/c$ .  $a = 5.4659(1)$  Å;  $b = 8.7272(2)$  Å;  $c = 9.7807(3)$  Å;  $\beta = 95.080(2)^\circ$ .

**TABLE 4**  
**Bond Lengths for  $\text{Li}_3\text{Cu}_2\text{SbO}_6$**

		Bond length (Å)		Bond angles (°)		
Li1	O1	2.075(18)	O1	Li1	O1	90.0(7)
	O1	2.145(18)	O1		O2	75.6(6)
	O2	2.36(2)	O1		O2	161(1)
	O2	2.069(18)	O1		O3	88.5(7)
	O3	2.188(19)	O1		O3	99.8(8)
	O3	1.97(2)	O1		O2	93.7(7)
			O1		O2	94.3(8)
			O1		O3	173(1)
			O1		O3	81.5(7)
			O2		O2	85.8(7)
			O2		O3	92.8(7)
			O2		O3	173(1)
			O2		O3	89.3(8)
			O2		O3	99.0(9)
		O3		O3	91.8(8)	
Li/Cu2	O1	2.623(4) × 2	O1	LiCu2	O1	180
	O2	2.032(8) × 2	O1		O2	89.1(3) × 2
	O3	2.024(7) × 2	O1		O2	90.9(3) × 2
			O1		O3	82.4(2) × 2
			O1		O3	97.6(2) × 2
			O2		O3	84.9(3) × 2
			O2		O3	95.1(3) × 2
			O2		O2	180
			O3		O3	180
	Li/Cu3	O1	2.038(8) × 2	O1	LiCu3	O1
O2		2.361(6) × 2	O1		O2	98.7(3) × 2
O3		2.083(9) × 2	O1		O2	78.3(3) × 2
			O1		O2	92.5(3) × 2
			O1		O3	164.8(3) × 2
			O2		O2	175.6(3)
			O2		O3	87.1(3) × 2
			O2		O3	86.1(3) × 2
			O3		O3	84.7(3)
Cu4	O1	2.141(8) × 2	O1	Cu3	O2	93.5(3) × 2
	O2	2.099(9) × 2	O1		O2	88.2(2)
	O3	2.489(5) × 2	O1		O2	169.3(3) × 2
			O1		O3	98.7(2) × 2
			O1		O3	77.8(2) × 2
			O2		O2	86.7(3)
			O2		O3	91.5(3) × 2
			O2		O3	92.0(3) × 2
			O3	Cu4	O3	175.2(2)
Sb5	O1	1.964(4) × 2	O2	Sb5	O3	87.9(3) × 2
	O2	2.003(8) × 2	O2		O1	87.0(3) × 2
	O3	1.941(8) × 2	O2		O1	89.3(3) × 2
			O2		O2	92.0(3)
			O2		O3	176.2(3) × 2
			O3		O1	86.9(3) × 2
			O3		O1	96.8(3) × 2
			O3		O3	92.6(3)
			O1		O1	174.6(3)

**TABLE 5**  
**Bond Valence Sums for  $\text{Li}_3\text{Cu}_2\text{SbO}_6$**

		Bond length	Bond valence	Cation valence	Valence sum
Li1	O1	2.07	0.198		
	O1	2.14	0.171		
	O2	2.36	0.108		
	O2	2.07	0.198	1.00	1.07
	O3	2.19	0.154		
	O3	1.97	0.244		
Li/Cu2	O1	2.622	0.073		
	O2	2.032	0.284	1.40	1.29
	O3	2.022	0.290		
Li/Cu3	O1	2.04(3)2	0.310		
	O2	2.36(2)2	0.145	1.60	1.47
	O3	2.08(3)2	0.282		
Cu4	O1	2.14(2)2	0.294		
	O2	2.10(3)2	0.325	2.00	1.48
	O3	2.49(2)2	0.122		
Sb5	O1	1.96(1)2	0.859		
	O2	2.00(3)2	0.761	5.00	5.07
	O3	1.94(2)2	0.914		

Within the structure, the  $\text{SbO}_6$  octahedra are isolated, maximizing the Sb–Sb distance and hence reducing repulsive forces. Each  $\text{SbO}_6$  shares edges with three  $\text{CuO}_6$  octahedra to form a hexagonal ring. The center of each ring is occupied by a  $\text{LiCu}(3)$  octahedron; the cations follow the sequence  $\text{LiCu}(3)\text{--Cu--Sb}$  along the  $b$ -axis. The hexagonal rings link to form sheets in the  $ab$  plane, Fig. 3a. The Jahn–Teller distortion in the  $\text{CuO}_6$  octahedra is compensated for by the regularity of the  $\text{SbO}_6$  octahedra, and hence the hexagonal rings are regular in shape and pack to form flat sheets, as can be seen in Fig. 3b.

The remaining cations are located between the  $\text{LiCu}(3)/\text{Cu/Sb}$  sheets. Again, hexagonal rings form in the  $ab$  plane, in this case from face-sharing  $\text{LiO}_6$  octahedra, with  $\text{LiCu}(2)$  located at the centers of the rings. For these layers, the cations follow the sequence  $\text{Li--Li--LiCu}(2)$  along the  $b$ -axis.

In  $\text{Li}_2\text{TiO}_3$ , the cation distribution alternates between layers of Li and layers of Li and Ti to give the overall cation stoichiometry of  $\text{Li}_2\text{Ti}$ . In  $\text{Li}_3\text{Cu}_2\text{SbO}_6$ , the distribution alternates between layers of Sb,  $\text{Li}_{0.4}\text{Cu}_{0.6}$ , Cu and layers of Li, Li,  $\text{Li}_{0.6}\text{Cu}_{0.4}$  to give the stoichiometry  $\text{Li}_3\text{Cu}_2\text{Sb}$ .

The magnetic susceptibility of  $\text{Li}_3\text{Cu}_2\text{SbO}_6$  was measured over the range 77–300 K; see Fig. 4. A weak magnetic signal was detected whose temperature dependence gave a linear plot of  $\chi^{-1}/T$  that extrapolated approximately to 0 K. The magnetic moment calculated from the slope was  $1.92\mu_{\text{B}}$  [9], and this, together with the linear Curie–Weiss plot, provides clear evidence for a paramagnetic structure containing  $\text{Cu}^{2+}$  ions.

The electrical conductivity of pressed, sintered pellets of  $\text{Li}_3\text{Cu}_2\text{SbO}_6$  was determined over the range 300–600 °C,

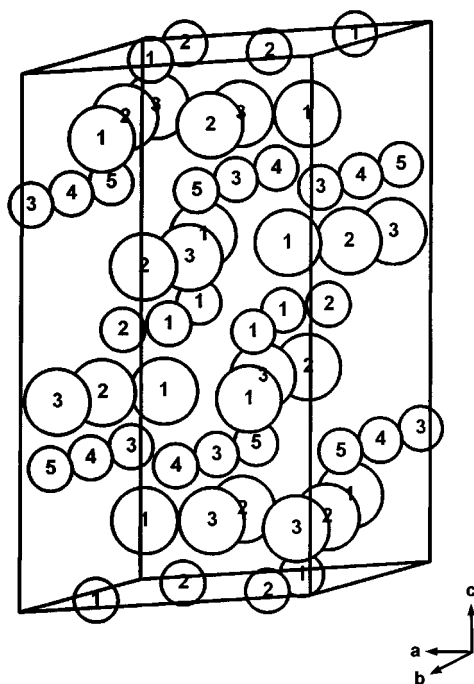


**FIG. 2.** The atom positions in the structure of  $\text{Li}_3\text{Cu}_2\text{SbO}_6$ . The numbers in the smaller circles indicate the cation sites: 1 = Li1, 2 = Li/Cu2, 3 = Li/Cu3, 4 = Cu4, and 5 = Sb5. Large circles are oxygens. This is related to the  $\text{Li}_2\text{TiO}_3$  structure, in which Li occupies sites 1–3 and Ti sites 4 and 5.

from analysis of variable frequency impedance data. The latter showed essentially a single, rather broadened arc in the complex impedance plane plot, with an associated capacitance of  $\sim 7$  pF indicating [10] that the measured impedance corresponded to the bulk of the sample rather than to grain boundary or surface layer effects. The absence

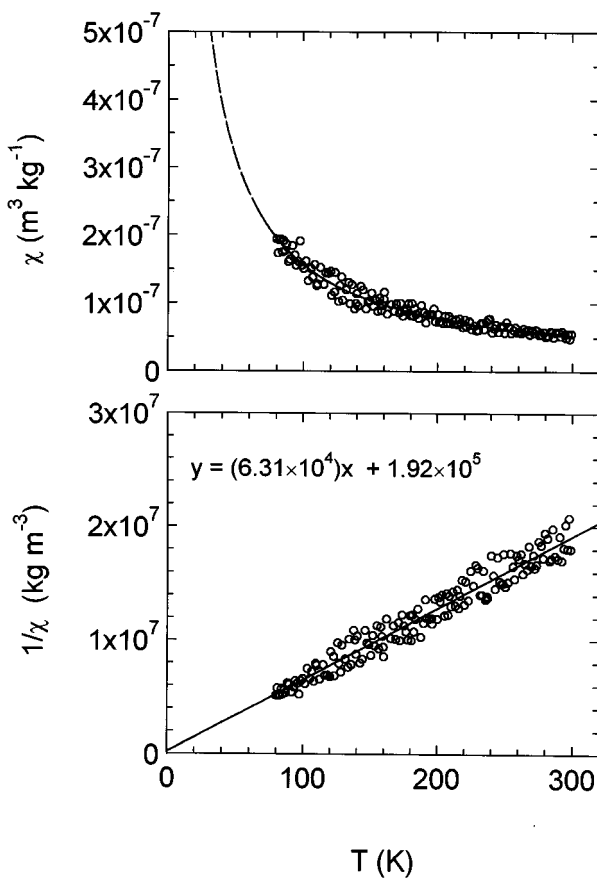
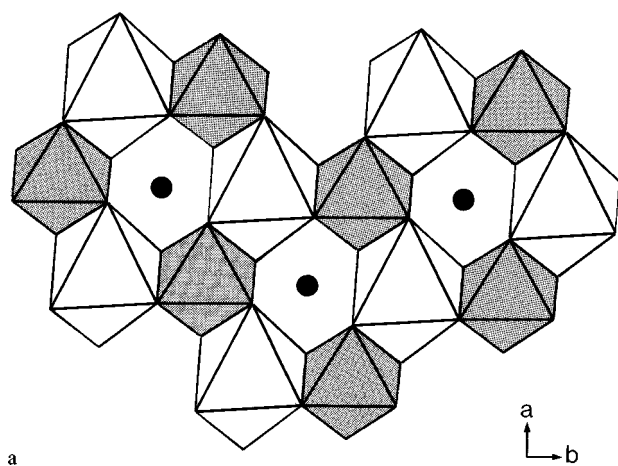


**FIG. 4.** Magnetic susceptibility data for  $\text{Li}_3\text{Cu}_2\text{SbO}_6$ .

of any low frequency, high capacitance effect indicated the absence of electrode polarization and therefore, that the conducting species is electronic rather than ionic. A conductivity Arrhenius plot is shown in Fig. 5; conductivity

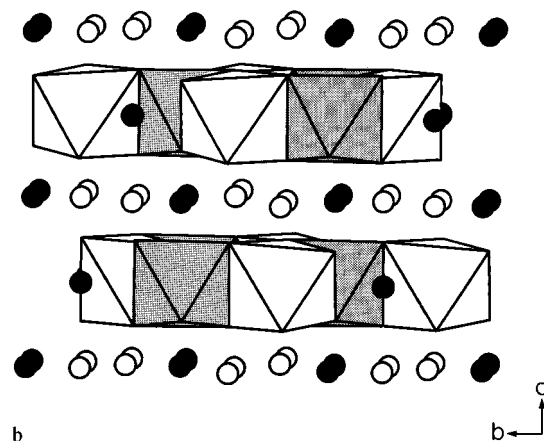


**FIG. 3.** (a) Hexagonal rings of  $\text{SbO}_6$  (shaded) and  $\text{CuO}_6$  (white) octahedra in the  $ab$  plane. Black circles are  $\text{Li}_{0.4}\text{Cu}_{0.6}$  atoms. (b) The layer structure of  $\text{Li}_3\text{Cu}_2\text{SbO}_6$  shown in the  $bc$  plane. Octahedra are as in the previous diagram; open circles are Li atoms, black circles are  $\text{Li}_{0.6}\text{Cu}_{0.4}$  atoms.

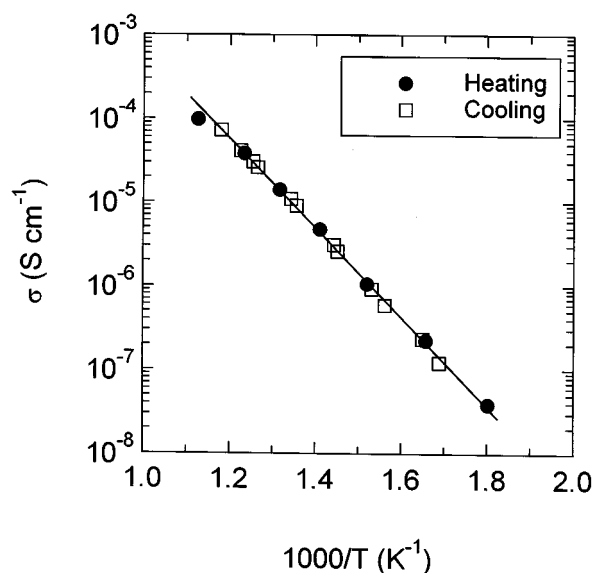


FIG. 5. Arrhenius plot of conductivity vs temperature for  $\text{Li}_3\text{Cu}_2\text{SbO}_6$ .

values are modest, e.g.,  $1 \times 10^{-7} \Omega^{-1} \text{cm}^{-1}$  at  $300^\circ\text{C}$  with an activation energy of 1.03 eV. Hence  $\text{Li}_3\text{Cu}_2\text{SbO}_6$  may be regarded as a very modest electronic semiconductor. This is not surprising given the green color of the sample, indicating the presence of electrically isolated  $\text{Cu}^{2+}$  ions.

## ACKNOWLEDGMENTS

We thank Dr. R. A. Howie for his assistance with bond length calculations, and we acknowledge the use of the EPSRC funded Chemical Database Service at Daresbury. MAC and STT thank UNAM for support through Project IN 101893 PAPIIT.

## REFERENCES

1. G. C. Mather, R. I. Smith, J. M. S. Skakle, J. G. Fletcher, M. A. Castellanos R., M. Pilar Gutierrez, and A. R. West, *J. Mater. Chem.* **5**, 1177 (1995).
2. J. G. Fletcher, G. C. Mather, A. R. West, M. A. Castellanos R., and M. P. Gutierrez, *J. Mater. Chem.* **4**, 1303 (1994).
3. G. C. Mather and A. R. West, *J. Solid State Chem.* **124**, 214 (1996).
4. S. Trujillo Tovar, M.Sc. Thesis, UNAM, Mexico, 1997.
5. J. M. S. Skakle, M. A. Castellanos R., S. Trujillo Tovar, S. M. Fray, and A. R. West, *J. Mater. Chem.* **6**, 1939 (1996).
6. M. A. Castellanos, S. Trujillo Tovar, J. M. S. Skakle, and A. R. West; in "Solid State Chemistry," MRS Symposium Proceedings, in press.
7. J. F. Dorian and R. E. Newnham, *Mater. Res. Bull.* **4**, 179 (1969).
8. I. D. Brown, in "Structure and Bonding in Crystals" M. O'Keefe and A. Navrotsky, Eds., vol. II, Academic Press, 1981.
9. C. Kittel, "Introduction to Solid State Physics," Wiley, New York, 1986.
10. J. T. S. Irvine, D. C. Sinclair, and A. R. West, *Adv. Mater.* **2**, 132 (1990).